Nakajima and Tanoue, http://www.jcb.org/cgi/content/full/jcb.201104118/DC1

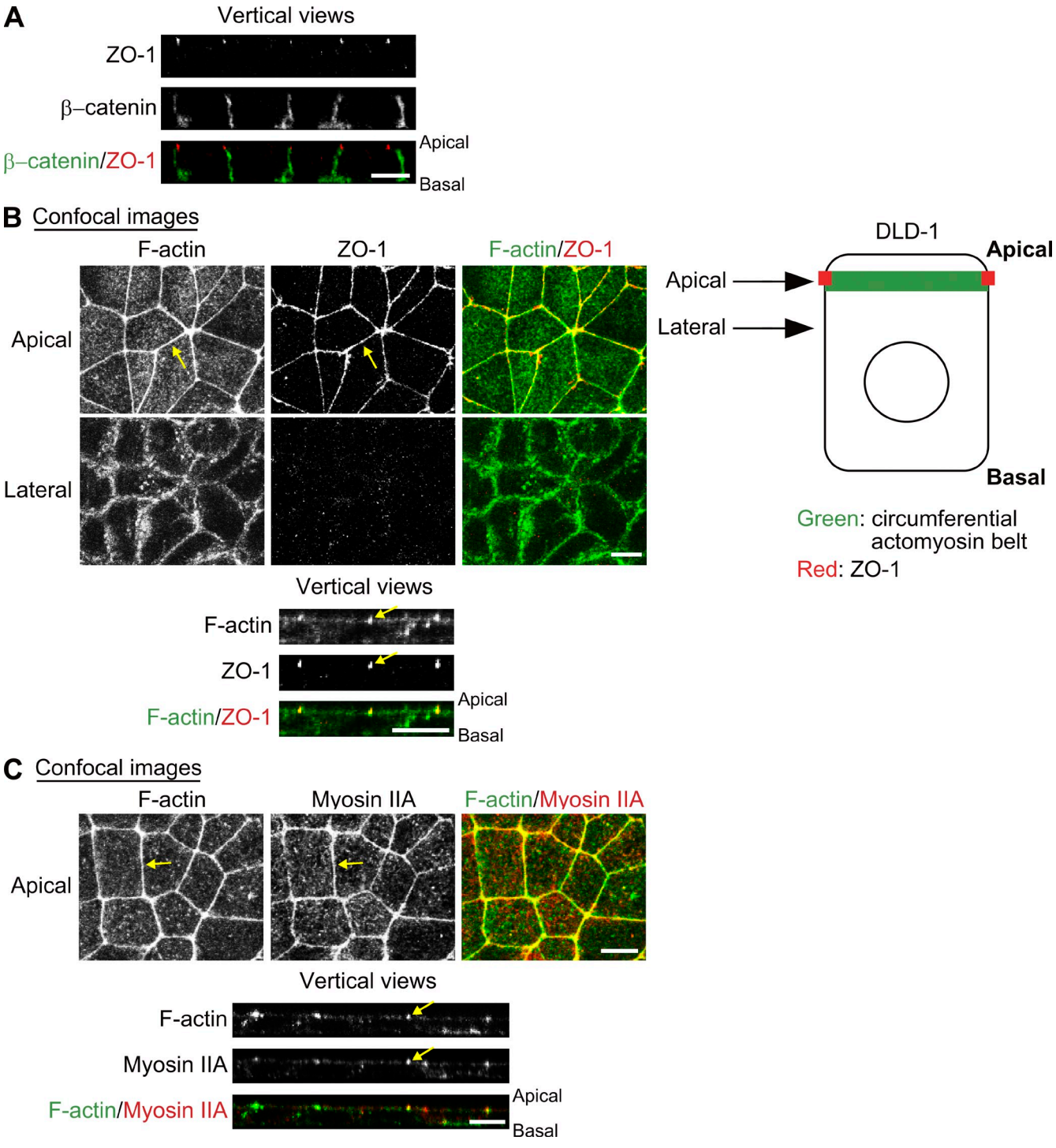

Figure S1. **DLD-1 cells exhibit the characteristic morphology of polarized epithelial cells with a well-developed circumferential actomyosin belt.** (A) DLD-1 cells doubly stained for ZO-1 and β-catenin. Vertical images are shown. ZO-1 accumulates at apical cell–cell boundaries, whereas β-catenin accumulates at the lateral membranes of the cells. (B) Confocal images of DLD-1 cells doubly stained for ZO-1 and F-actin at top and middle levels. The circumferential actomyosin belt indicated by F-actin staining is localized along apical cell–cell boundaries marked by ZO-1 (arrows). At the lateral membranes, F-actin staining exhibits fibrous structures. (C) DLD-1 cells doubly stained for F-actin and myosin IIA. The circumferential actomyosin belt is localized along apical cell–cell boundaries (arrows). Bars, 10 µm.

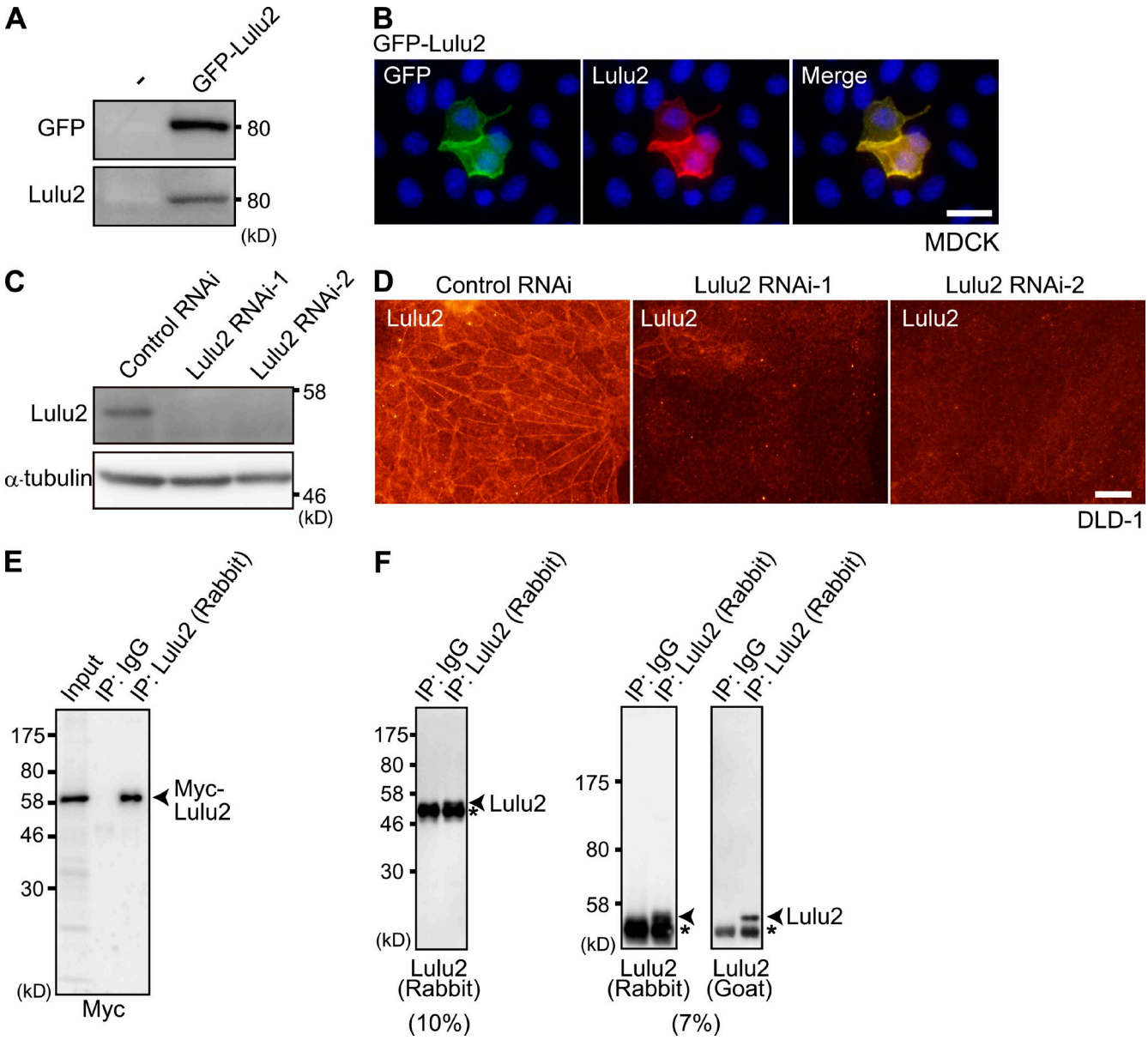

Figure S2. **Characterization of the anti-Lulu2 antibodies.** (A) Lysates of parental MDCK cells or MDCK cells transiently expressing EGFP-Lulu2 were analyzed by immunoblotting with anti-GFP antibody or the goat anti-Lulu2 antibody. This antibody detected EGFP-Lulu2. In MDCK cells, endogenous Lulu2 was scarcely detected (not depicted). Minus sign indicates no transfection. (B) MDCK cells transiently expressing EGFP-Lulu2 were doubly immunostained with anti-GFP and the anti-Lulu2 antibodies. The staining signal of the anti-Lulu2 antibody was identical to that of the anti-GFP antibody. Nuclei were visualized with DAPI. (C) DLD-1 cells were transfected with control siRNA, Lulu2 siRNA-1, or Lulu2 siRNA-2 (see Materials and methods), subjected to immunoprecipitation using the anti-Lulu2 antibody, and then analyzed by immunoblotting with the anti-Lulu2 antibody. This anti-Lulu2 antibody is very weak for using in immunoblotting. Lulu2 siRNA-1 and -2 efficiently knocked down Lulu2 expression. (D) DLD-1 cells treated with control siRNA, Lulu2 siRNA-1, or Lulu2 siRNA-2 were immunostained with the anti-Lulu2 antibody. Lulu2 expression is efficiently knocked down by Lulu2 siRNAs. (E and F) Characterization of the rabbit anti-Lulu2 antibody used in the coimmunoprecipitation (IP) assay in Fig. 2 D. The antibody was raised against the mouse Lulu2/Ehm2 peptide (451–466 aa). Although this antibody is very weak for using in Western blotting and immunostaining to detect endogenous Lulu2, it can be used for the immunoprecipitation of endogenous Lulu2. Myc-tagged Lulu2 proteins expressed in MDCK cells were efficiently immunoprecipitated with the antibody but not control rabbit IgG (E), indicating that Lulu2 protein can be immunoprecipitated with the antibody. (E) Immunoprecipitated Myc-tagged Lulu2 was detected by anti-Myc antibody. (F) Lysates of DLD-1 cells were subjected to immunoprecipitation using control rabbit IgG or the anti-Lulu2 antibody. Immunoprecipitated endogenous Lulu2 was detected by the antibody (rabbit) or goat anti-Lulu2 antibody (goat). These antibodies commonly detected a band of ~55 kD in the immunoprecipitant, which might correspond to endogenous Lulu2 in DLD-1 cells. Asterisks indicate the heavy chains of the antibodies. Western blots using a 10 or 7% gel are shown. Bars, 20 μm.

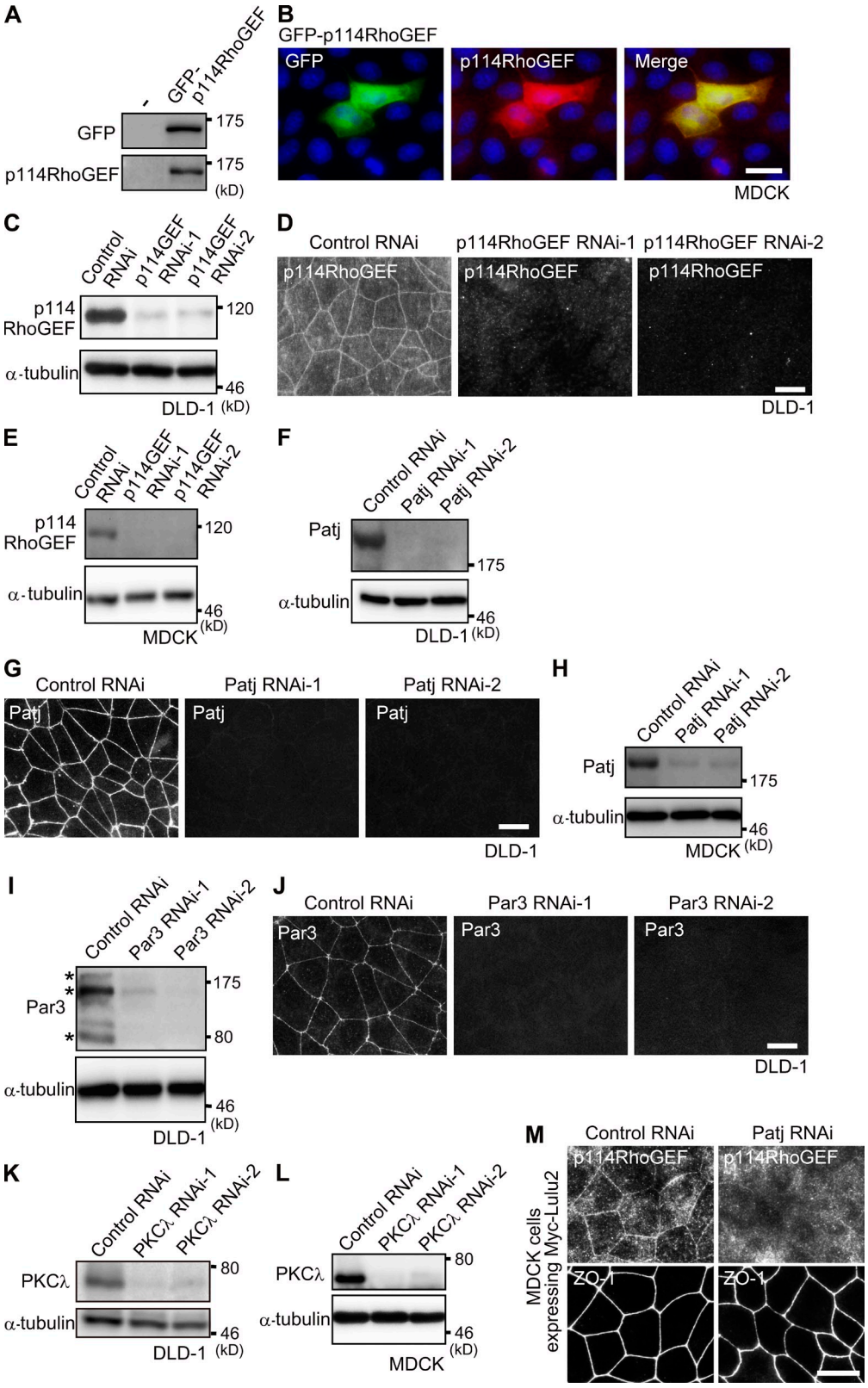

Figure S3. **Efficient knockdown of p114RhoGEF, Patj, Par3, and aPKC.** (A) Lysates of MDCK cells transiently expressing EGFP-p114RhoGEF were analyzed by immunoblotting with the anti-GFP antibody or anti-p114RhoGEF antibody. This antibody detected EGFP-p114RhoGEF. The minus sign indicates no transfection. (B) MDCK cells transiently expressing EGFP-p114RhoGEF were doubly immunostained with anti-GFP and the anti-p114RhoGEF antibodies. The staining signal of the anti-p114RhoGEF antibody was identical to that of the anti-GFP antibody. Nuclei were visualized with DAPI. (C–L) p114RhoGEF (C–E), Patj (F–H), Par3 (I and J), or PKC-λ (K and L) was efficiently knocked down by siRNAs in DLD-1 (C, D, F, G, and I–K) or MDCK (E, H, and L) cells. Western blots or immunostaining images are shown. α-Tubulin was a loading control. See Materials and methods for siRNAs. Par3 has three spliced forms (asterisks in I). (M) MDCK cells treated with control siRNA or Patj siRNA-1 were stained for p114RhoGEF and ZO-1. p114RhoGEF mostly disappeared from cell–cell boundaries in Patj-depleted MDCK cells. See Materials and methods for siRNAs. Bars, 20 μm.

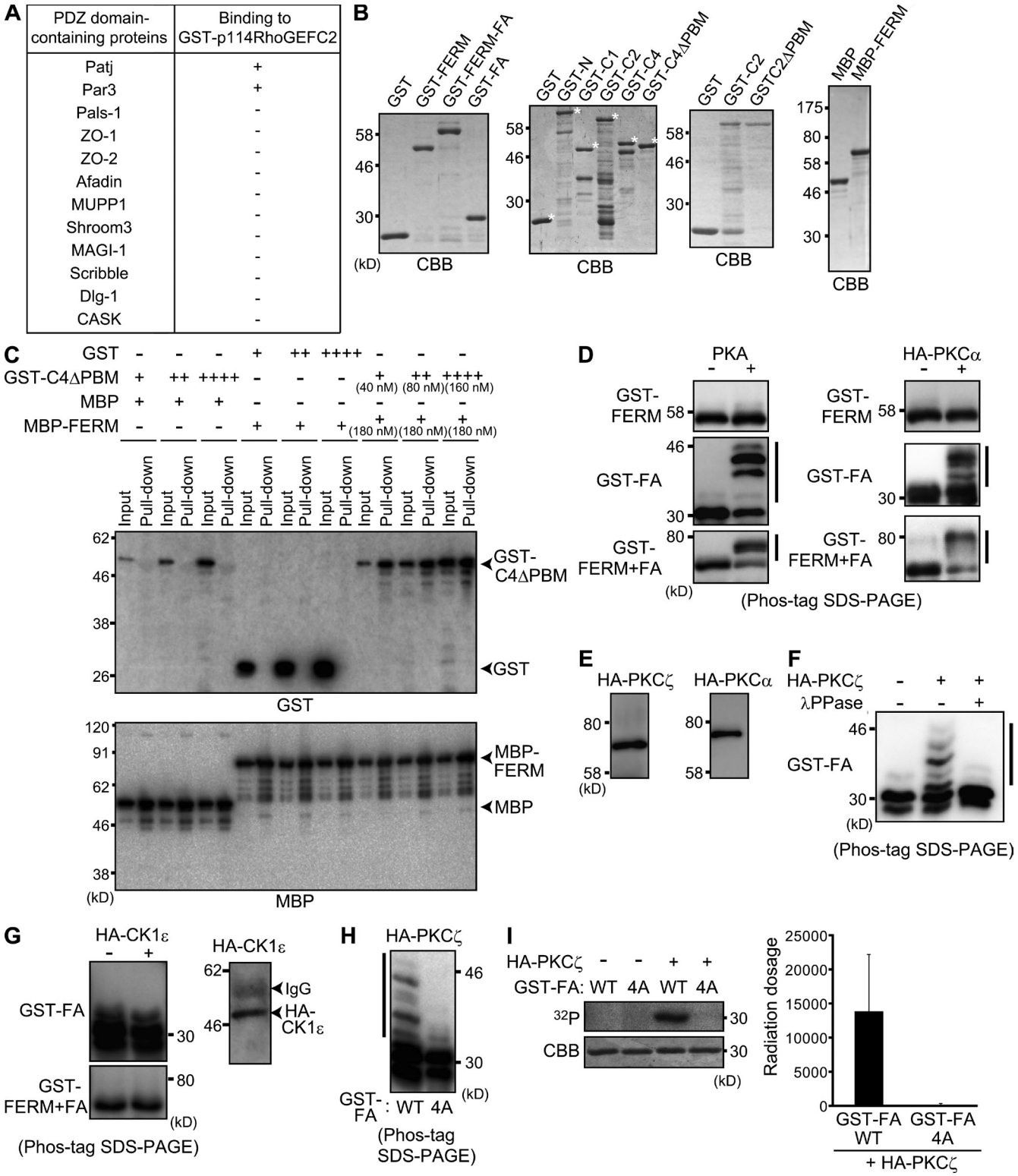

Figure S4. **p114RhoGEF binds to Patj and Par3.** (A) Several PDZ domain–containing molecules known to be localized along cell–cell boundaries were examined for binding to the C2 region of p114RhoGEF by GST pull-down assays. GST-p114RhoGEFC2 was used. The results are shown in the table (+, bound; −, unbound). p114RhoGEFC2 bound to Par3 and Patj. (B) GST proteins used in this study were stained by CBB. Asterisks show full-length proteins. (C) p114RhoGEF C4ΔPBM was tested for binding to the FERM domain of Lulu2 in vitro in various concentrations. GST-fused C4ΔPBM (40 [+], 80 [++], or 160 [++++] nM) or GST (160 [+], 320 [++], or 580 [++++] nM) was mixed and incubated with MBP-fused FERM (180 nM) or MBP (180 nM) and precipitated with amylose resin (MBP pull-down). Precipitated proteins were detected by immunoblotting using anti-MBP or -GST antibodies. In these three concentrations, GST-C4ΔPBM, but not GST, efficiently binds to MBP-FERM, but not MBP, indicating that the FERM domain binds to C4ΔPBM in vitro. (D) GST-FERM-FA, GST-FERM domain, and GST-FA domain (1 μg each) were subjected to in vitro kinase assays with the catalytic subunit of PKA purified from bovine heart (Sigma-Aldrich) or eluted HA–PKC-α (used in E). 1 U PKA protein was used. PKA and PKC-α efficiently phosphorylates GST-FERM-FA and GST-FA but not GST-FERM. (E) HA–PKC-ζ and HA–PKC-α used in Fig. 7 B and panel D of this figure. HA–PKC-ζ (left)

or HA–PKC-α (right) was eluted using HA peptides from immunoprecipitants from MDCK cells expressing HA–PKC-ζ or HA–PKC-α and then analyzed by immunoblotting with the anti-HA antibody. (F) Confirmation of the phosphorylation of GST-FA domain by aPKC. 1 µg GST-FA was phosphorylated by HA–PKC-ζ, and then left untreated or treated with 800 U λ protein phosphatase (λPPase; New England Biolabs, Inc.) for 45 min at 30°C. λ protein phosphatase treatment results in complete loss of the band shift, confirming that the shift indicates phosphorylation of GST-FA. (G) CKI-ε, which has different substrate preference, did not cause a mobility retardation of the FA domain in the assay, suggesting the specificity of PKCs and PKA. GST-FERM-FA and GST-FA domain (1 µg each) were subjected to in vitro kinase assays with HA–CKI-ε. (right) The HA–CKI-ε used is also shown. CKI-ε did not phosphorylate GST-FERM-FA and GST-FA domain. (H) GST-FA domain and GST-FA 4A, in which four aPKC phosphorylation sites (Ser385, Ser414, Ser419, and Thr424) were replaced by alanines, were subjected to in vitro kinase assays with HA–PKC-ζ. PKC-ζ phosphorylated GST-FA (wild type [WT]) but not GST-FA 4A in vitro. (D, F, G, and H) Phosphorylation was detected by mobility shift patterns (bars) in Mn^{2+}–Phos-tag SDS-PAGE followed by immunoblotting with anti-GST antibody. (I) GST-FA domain and GST-FA 4A were subjected to in vitro kinase assays with HA–PKC-ζ. Phosphorylation was detected as incorporation of γ-[^{32}P] ATP (PerkinElmer). 3 µg GST-FA or 3 µg GST-FA 4A were mixed with eluted HA–PKC-ζ in kinase reaction buffer (20 mM Tris-HCl, pH 7.5, 10 mM $MgCl_2$, and 100 µM ATP [2 µCi of γ-[^{32}P]ATP]) and incubated for 30 min at 37°C. The reaction was stopped by the addition of Laemmli sample buffer. Substrate phosphorylation was detected by autoradiography and with a molecular imager (BAS-2500; Fujifilm) after SDS-PAGE. PKC-ζ phosphorylated GST-FA (wild type) but not GST-FA 4A in vitro. (right) Measurement of radiation dosage of three independent experiments is also shown. Error bars indicate SD.

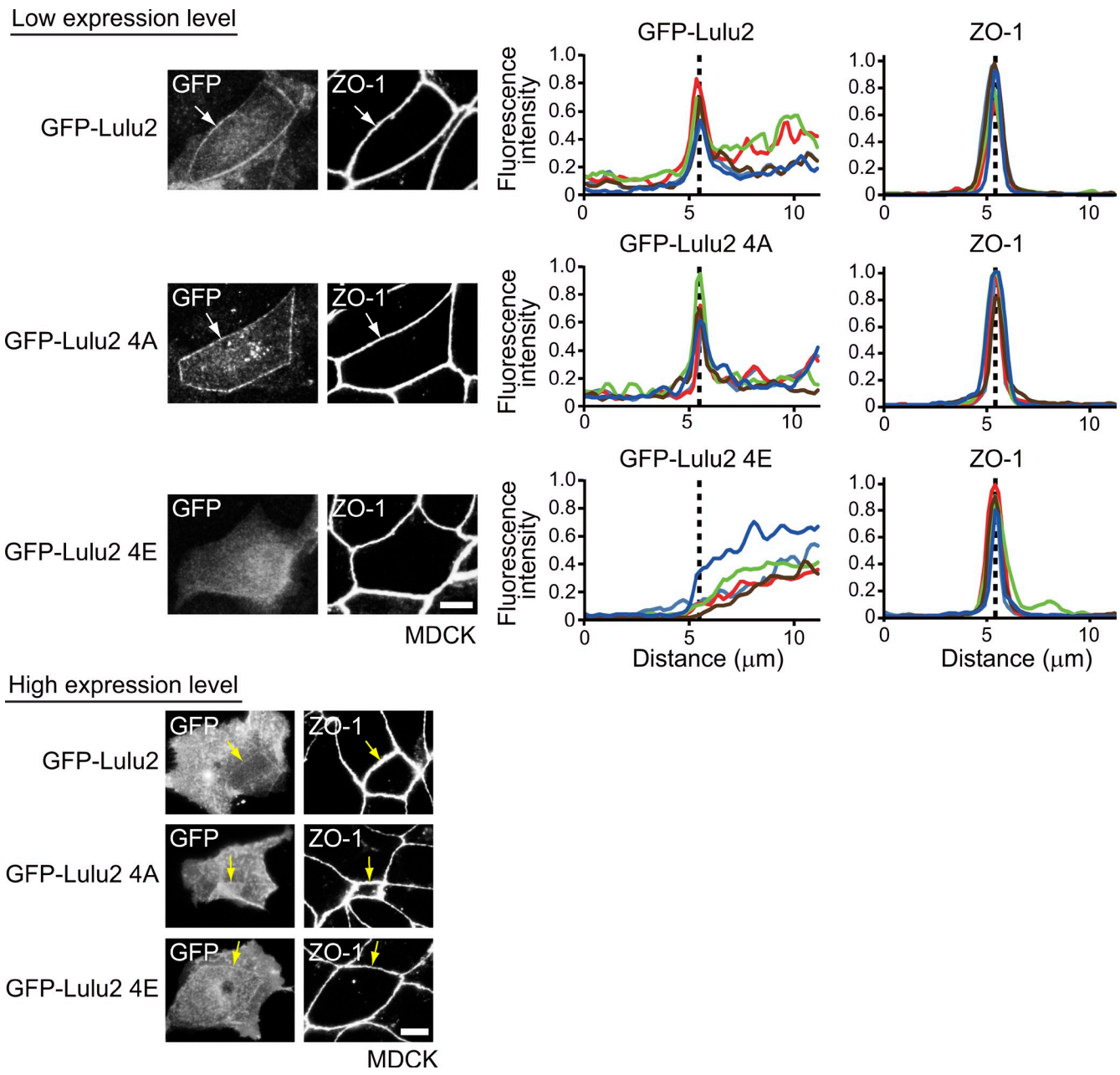

Figure S5. **Lulu2 4A accumulated along cell–cell boundaries, whereas Lulu2 4E did not.** MDCK cells transfected with EGFP-tagged wild-type Lulu2, Lulu2 4A, or Lulu2 4E were doubly immunostained for EGFP and ZO-1. Apical portions of the cells are focused. Fluorescence intensity of the EGFP or ZO-1 signal was scanned across cell–cell boundaries between control and EGFP-expressing cells (left and right of dotted lines, respectively). Five different cell–cell boundaries were measured (shown in different colors). Wild-type Lulu2 and Lulu2 4A accumulated along cell–cell boundaries overlapping ZO-1 (white arrows), whereas Lulu2 4E did not. Note that the cells at very low expression levels of each molecule were examined. Because of the low expression, apical constriction was not observed even in wild-type Lulu2-expressing cells. (bottom) In the cells expressing Lulu2 4E at higher expression levels, Lulu2 4E also accumulated along cell–cell boundaries overlapping ZO-1 like wild-type Lulu2 and Lulu2 4A (yellow arrows). Bars, 10 μm.